Available online at www.sciencedirect.com

SCIENCE DIRECT®

Biochimica et Biophysica Acta 1659 (2004) 63–72

BIOCHIMICA ET BIOPHYSICA ACTA
BBA

http://www.elsevier.com/locate/bba

Plastocyanin redox kinetics in spinach chloroplasts: evidence for disequilibrium in the high potential chain

Helmut Kirchhoff*, Mark Aurel Schöttler, Julia Maurer, Engelbert Weis

Institut für Botanik, Schlossgarten 3, D-48149 Münster, Germany

Received 24 May 2004; received in revised form 9 August 2004; accepted 12 August 2004
Available online 26 August 2004

Abstract

Reduction kinetics of cytochrome *f*, plastocyanin (PC) and P_{700} ('high-potential chain') in thylakoids from spinach were followed after pre-oxidation by a saturating light pulse. We describe a novel approach to follow PC redox kinetics from deconvolution of 810–860 nm absorption changes. The equilibration between the redox-components was analyzed by plotting the redox state of cytochrome *f* and PC against that of P_{700}. In thylakoids with (1) diminished electron transport rate (adjusted with a cytochrome *bf* inhibitor) or (2) de-stacked grana, cytochrome *f* and PC relaxed close to their thermodynamic equilibriums with P_{700}. In stacked thylakoids with non-inhibited electron transport, the equilibration plots were complex and non-hyperbolic, suggesting that during fast electron flux, the 'high-potential chain' does not homogeneously equilibrate throughout the membrane. Apparent equilibrium constants <5 were calculated, which are below the thermodynamic equilibrium known for the 'high potential chain'. The disequilibrium found in stacked thylakoids with high electron fluxes is explained by restricted long-range PC diffusion. We develop a model assuming that about 30% of Photosystem I mainly located in grana end-membranes and margins rapidly equilibrate with cytochrome *f* via short-distance transluminal PC diffusion, while long-range lateral PC migration between grana cores and distant stroma lamellae is restricted. Implications for the electron flux control are discussed.

Keywords: Plastocyanin; Redox equilibrium; Thylakoids; Diffusion

1. Introduction

In higher plants, most algae and some cyanobacteria, the blue copper-protein plastocyanin (PC) mediates the photosynthetic electron transport (ET) between the membrane-embedded complexes cytochrome (cyt) *bf* complex and Photosystem (PS) I [1]. PC is localized in the thylakoid lumen. Its structure is known at atomic resolution [2]. The kinetics of the electron transfer between cytochrome *f*, PC and PSI and its structural basis are well known [3,4]. Tight encounter-complexes between PC and its docking sites at the cyt *bf* complex and PSI are formed, which allow very rapid electron transfer from the heme complex of cytochrome *f* to the PC copper complex (time constant 35–350 μs) and from PC to P_{700} (time constant 10–20 μs; [3]), respectively. However, to carry electrons between distant cyt *bf* complexes and PSI, the small (10 kDa) PC protein must migrate throughout the thylakoid lumen between protruding protein complexes [4]. The influence of the lumen structure on the PC diffusion is still not clear.

The thylakoid lumen is enclosed by the partially stacked thylakoid membrane, forming distinct subcompartments. Grana exhibit strictly stacked membranes ('grana core') and 'exposed' grana membrane regions, such as the bent margins and the flat end-membranes [5]. The grana are interconnected by unstacked stroma lamellae. The protein complexes involved in the photosynthetic energy transduction are asymmetrically distributed between these sub-

Abbreviations: chl, chlorophyll; cyt, cytochrome; DNP-INT, 2,4-dinitrophenylether of iodonitrothymol; $\Delta\varepsilon$, differential absorption coefficient; E_m, redox midpoint potential; ET, electron transport; FR, far red; P_{700}, reaction centre chlorophyll of Photosystem I; PAM, pulse-amplitude-modulation; PC, plastocyanin; PQ, plastoquinone; PS, photosystem

* Corresponding author. Tel.: +49 251 832 4820; fax: +49 251 832 3823.
E-mail address: kirchhh@uni-muenster.de (H. Kirchhoff).

0005-2728/$ - see front matter © 2004 Elsevier B.V. All rights reserved.
doi:10.1016/j.bbabio.2004.08.004

compartments [6]. PSII with LHCII are preferentially located in the grana core, whereas PSI, LHCI and the ATPase are excluded from this area and are located in exposed grana membranes and stroma lamellae. It is assumed that the cyt *bf* complex is more or less equally distributed throughout the membrane, i.e. one fraction of this complex is located in exposed regions, adjacent to PSI, another fraction in inner grana regions, distant to PSI. Grana stacks exhibit a diameter of 400–500 nm [7]. It was calculated that the mean distance between half of cyt *bf* complexes located in the grana core and PSI is 60–70 nm (assuming random cyt *bf* distribution, [8]). Furthermore, the inner width of the thylakoid lumen (approx. 4 nm, [5]) and the size of the PC protein (approx. 4×3×3 nm, [2]) are in the same order. In addition, it is assumed that the luminal width can be further reduced in illuminated chloroplasts [9]. Haehnel et al. [10] could clearly demonstrate that PC does diffuse in the light from the distant stroma lamellae to the grana core, but it was questioned whether this long-distance PC migration could be fast enough to support the linear electron transport, which requires transfer rates in the order of 10 ms [8,11]. Recently, it was reported that a decline in the width of the thylakoid lumen by hyperosmotic stress actually slowed the electron transport rate from PC to P_{700}^{+} in *Chlamydomonas* down, suggesting that the luminal width could affect PC diffusion [12]. In addition, a large number of protruding parts of grana protein complexes such as the extrinsic proteins of the water splitting complex of PSII [13] and cytochrome *f* [14] could act as diffusion obstacles and are likely to contribute to a restriction of the PC diffusion. On the other hand, PC diffusion is facilitated by the two-dimensional character of the diffusion space, and its docking to the target proteins, cytochrome *f* and the PsaF subunit of PSI, is supported by long-range electrostatic attraction [3].

The control of long-distance migration of PC could be of significance for the appropriate matching of the light-driven linear electron transport to PSI and the electron-consuming metabolic reactions. It could also affect the balance between linear and cyclic electron transport. If cyclic transport is located in stroma lamellae (e.g. Ref. [6]), this compartment should be protected from rapid redox equilibration with PSII in the grana stacks, i.e. fast PC migration from inner grana stacks to the distant stroma lamellae could disturb the redox poising needed for cyclic transport [15]. Overall, long-distance migration of PC is an important problem regarding the control of photosynthetic electron transport. There exists a number of arguments in favour of restricted PC diffusion. Yet, there is still no clear concept integrating PC diffusion and the control of electron transport. Interestingly, there is increasing evidence that the PC gene (*petE*) expression is highly regulated by various environmental factors [16,17]. By this regulation, PC could be adjusted to changing metabolic conditions.

In this work, we analyze redox kinetics of the components of the 'high potential chain', cytochrome *f*, PC and P_{700}. A novel approach to measure redox kinetics of PC from absorption changes in the 810–860 nm range (measured with a pulse-amplitude-modulation (PAM) photometer) is described. In saturating light pulses, the 'high potential chain' becomes fully oxidized. We measured and compared the reduction of the three redox components in the dark after the light pulse, reflecting the redox equilibration between these components. We demonstrate that the components of the 'high potential chain' remain far from their thermodynamic equilibrium and suggest that only a minor fraction of PC, located in the outer regions of grana, could rapidly equilibrate with adjacent cyt *bf* complexes and PSI. The long-distance PC migration between grana cores and distant membrane regions, however, is relatively slow and hinders redox-equilibration throughout the membrane. We discuss our observations in the light of the flux control of the linear electron transport and the balance between linear and cyclic flux.

2. Materials and methods

2.1. Preparations

Chloroplasts were isolated from 6-week-old leaves of spinach (*Spinacea oleracea* var. *polka*) grown in a hydroponics medium [18] at 13–16 °C according to Ref. [19]. The photoperiod was 10 h (300 μmol quanta m^{-2} s^{-1}). The chlorophyll content was determined according to Ref. [20].

PSI enriched particles were isolated according to Ref. [21]. The P_{700} content increased from 2.0 to 3.0 mmol/mol chl, indicating that the preparation still contained PSII and LHCII. However, for our purpose, it was important that the preparation no longer contained any PC. This was ensured by the isolation protocol. A PC-enriched preparation was isolated from thylakoid membranes washed twice in a buffer containing 100 mM sorbitol, 10 mM NaCl, 10 mM $MgCl_2$, 30 mM HEPES (pH 7.8, KOH), and 2 M NaBr to remove peripheral proteins localized at the stroma side of the membrane, namely ferredoxin. Membranes treated in this way were subjected to 10 cycles of freezing and thawing in order to release PC from the lumen [22]. The membranes were pelleted (35,000×*g*, 20 min) and the PC containing supernatant was concentrated with a Centricon 10 (cut-off 10 kDa). The purity of the PC preparation and the absence of ferredoxin were checked by comparison of difference absorption spectra (1 mM ferricyanide minus 10 mM sodium ascorbate) with literature spectra [23,24]. The measurements were made with a Hitachi U3010 photometer (slit width 1 nm, 300 nm/min).

2.2. Spectroscopy

Redox kinetics of cytochrome *f* were obtained from difference absorption signals in the green wavelength region (545, 554 and 575 nm) in a self-constructed photometer as described in Ref. [19]. The measuring beam was produced

by a Bausch and Lomb monochromator. Saturating 100 ms red light pulses (about 5 mmol quanta per m^2 and s, 630 nm) generated by a high power LED cone (Walz Company, Effeltrich, Germany) were directed into the cuvette perpendicular to the measuring beam via fiber optics. In the third optical axis, PC^+ and P_{700}^+ were followed in the far red (FR). The pulse-modulated (100 kHz) FR measuring beam was produced and signals were collected by a PAM 101 photometer (Walz) with the emitting-detecting units ED-800T (810 nm) [23] and ED-P700DW (810–860 nm) [25]. FR signals were recorded simultaneously with the cytochrome *f* signals. Fifteen measurements for each signal were averaged (repetition frequency 3 s). The deconvolution procedure is described in Results.

Shortly before the measurements, the chloroplast envelope was removed by a 30-s osmotic shock in a hypotonic medium. During the measurements, the suspension medium contained 300 mM sorbitol, 50 mM KCl, 7 mM $MgCl_2$ and 30 mM HEPES, pH 7.6 (KOH) and thylakoid membranes equivalent to 30 μM chlorophyll. Methylviologen (50 μM), nigericin (1 μM), nonactin (0.5 μM) and sodium ascorbate (1 mM) were added. 2,4-Dinitrophenylether of iodonitrothymol (DNP-INT) was added as indicated. For de-stacking, thylakoids were transferred in 10 mM KCl and 15 mM HEPES, pH 7.6 (KOH).

For FR absorbance measurements with leaves, 1.8 cm discs from spinach leaves were infiltrated with tap water containing 0.4 mM methylviologen. Five minutes after infiltration the leaf discs were placed in a reflecting cuvette. The modulated measuring beam, the measuring signals and a 120 ms red light pulse (5 mmol quanta per m^2 and s, 645–700 nm) were guided via a threefold-branched fiber optics through the cuvette.

3. Results

3.1. Deconvolution of FR absorbance changes in PC and P_{700} redox kinetics

P_{700}^+ and PC^+ signals were obtained from FR difference signals at (860–810 nm; ED-P700DW unit) and at 810 nm (ED-800T unit). The differential absorption coefficients required for the deconvolution of the absorption signals are summarized in Table 1. The values were determined from PSI- or PC-enriched preparations (see Materials and methods). The PC content of the preparation was obtained from the absorption difference spectrum at 597 nm (ferricyanide minus sodium ascorbate) using an absorption coefficient $\Delta\varepsilon$=4.9 mM^{-1} cm^{-1} [24]. The P_{700}^+ concentration was obtained from light-pulse induced difference signals at 702 nm (see Ref. [19]). Using suspensions of either PC- or PSI-enriched preparations with adjusted chromophore concentrations, we determined the apparent absorption coefficients for our measuring system (Table 1). Assuming a PC/P_{700} ratio of 3:4 in thylakoid membranes

Table 1
Differential absorption coefficients, $\Delta\varepsilon$, of PC and P_{700} for the FR measuring heads

	$\Delta\varepsilon$ 810 nm	$\Delta\varepsilon$ (810–860 nm)
PC	1.59 mM^{-1} cm^{-1}	0.44 mM^{-1} cm^{-1}
P_{700}	10.30 mM^{-1} cm^{-1}	9.60 mM^{-1} cm^{-1}

(see below) it follows from the $\Delta\varepsilon$ values in Table 1, that the contamination of the 'P_{700} signal' (810–860 nm) signal with the PC-dependent signal is between 12% and 15%. At 810 nm, the contribution of PC was estimated to be 32–38% of the total amplitude. On the basis of Table 1, Eqs. (1) and (2) were used to deconvolute FR absorbance changes in its PC and P_{700} redox signals.

$$c_{PC} = \frac{\Delta A_{810} 9.60 - \Delta A_{810-860} 10.30}{d 10.73} \quad (1)$$

$$c_{P_{700}} = \frac{\Delta A_{810-860} 1.59 - \Delta A_{810} 0.44}{d 10.73} \quad (2)$$

c_{PC}, $c_{P_{700}}$, concentration of PC and P_{700} in mM; ΔA_{810}, $\Delta A_{810-860}$, absorption change at 810 or 810–860 nm; d, optical path length in cm.

Fig. 1 shows an example for a deconvolution of light pulse-induced FR absorption changes measured with isolated thylakoid membranes. The presence of the PSI electron acceptor methylviologen [26] and the uncouplers nigericin and nonactin suppress ΔpH- and Δψ-dependent light scattering changes [23]. Sodium ascorbate was added to keep the 'high potential chain' completely reduced in the dark. The saturating light pulse of 100 ms (grey bar in Fig. 1, left) quantitatively oxidizes the 'high potential chain'. Thus, the ratio PC/P_{700} can be derived from the maximal signal changes (Fig. 1, right). A PC/P_{700} of 3.60±0.35 (n=5) was calculated, which is in good agreement with values published for spinach [10,23]. The validity of the deconvolution procedure was further proved and confirmed by repeating the measurements with thylakoids where PC was either inactivated by KCN treatment [22] or released from thylakoids by freezing–thawing cycles [22]. As expected, the absorption changes induced by the treatments corresponded well with the predicted changes from Table 1 (not shown).

In the light pulse, P_{700} reached a nearly oxidized state within about 20 ms. A rapid initial photooxidation of PC (about three-fourths) was followed by a slow oxidation phase (about one-fourth), which was nearly (about 95% oxidation) completed at the end of the light pulse (100 ms). Similarly, the PC^+ relaxed more slowly in the dark compared to P_{700}^+. In thylakoid preparations, the P_{700}^+ relaxation signal usually showed a small slow component (time constant >150 ms; Fig. 1, right). Its amplitude varied with preparations from 10% to 20% of the total signal amplitude, but drastically increased in thylakoids exposed to freezing–thawing cycles (not shown). On the other hand, it was completely absent in intact leaves (see below). Thus, we conclude that the slow component represents a fraction

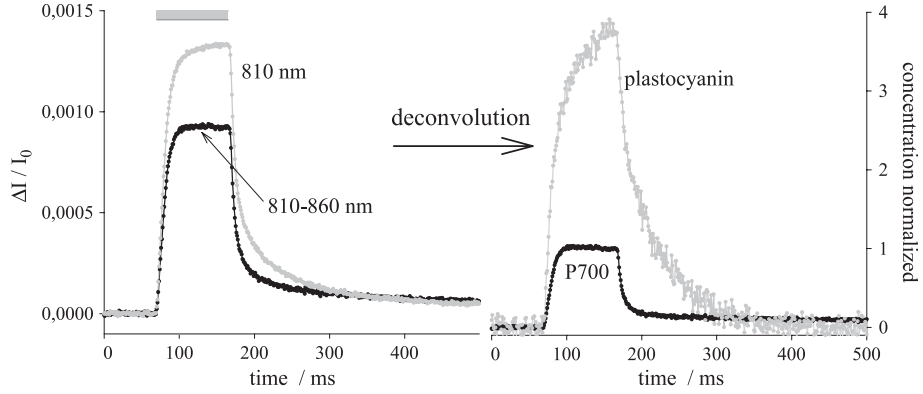

Fig. 1. Deconvolution of FR absorbance changes in P_{700} and PC redox kinetics. P_{700} and PC redox signals were calculated with Eqs. (1) and (2). The grey bar (left) indicates the saturating light pulse. Both deconvoluted redox signals (right) are normalized to the maximal P_{700} amplitude.

of PC-depleted thylakoids. It could be an artefact resulting from the isolation or osmotic shock procedure. We eliminated this component in the following equilibrium analysis.

3.2. Redox equilibration between cytochrome f, PC and P_{700} during the dark relaxation

At the end of the light pulse in Fig. 1, the 'high potential chain' is completely oxidized, whereas the plastoquinone (PQ) pool is highly reduced (redox cross-over). This is due to the rate-limiting step at the cyt *bf* complex [11]. In the following dark phase, electrons from the PQH_2-pool will pass the cyt *bf* complex and enter the 'high potential chain'. The redox equilibration within the 'high potential chain' can be examined by comparing the relaxation of the three components, cyt f^+, PC^+ and P_{700}^+ after the light pulse. Normalized values (100% photooxidized=1; 100% reduced state=0) for PC^+ and cyt f^+ obtained from these relaxation curves were plotted against P_{700}^+ (Fig. 2). In the following these plots in Fig. 2 are called 'equilibration plot'. Values around 1/1 represent the condition immediately after the light pulse where all components are highly oxidized. With increasing dark time, the relative proportion of the oxidized population decreases. At the 0/0 point, all components are reduced. Theoretical equilibrium curves (K_{eq}) are plotted in Fig. 2 (shaded area) calculated from published midpoint potentials (E_m) of cytochrome *f*, PC and P_{700} of spinach derived from equilibrium redox titrations (Table 2). These calculated curves represent the situation expected if the components of the 'high potential chain' would interact homogeneously, rapidly and close to their thermodynamic equilibrium.

The apparent equilibration plots derived from measured redox kinetics clearly differ from the calculated curves: Overall, the apparent equilibrium values (K_{app}) are significantly smaller than expected from the K_{eq} values. This suggests that the electron transfer from PC to PSI is restricted in such a way that PC and P_{700} do not equilibrate rapidly and P_{700} stays more oxidized than expected.

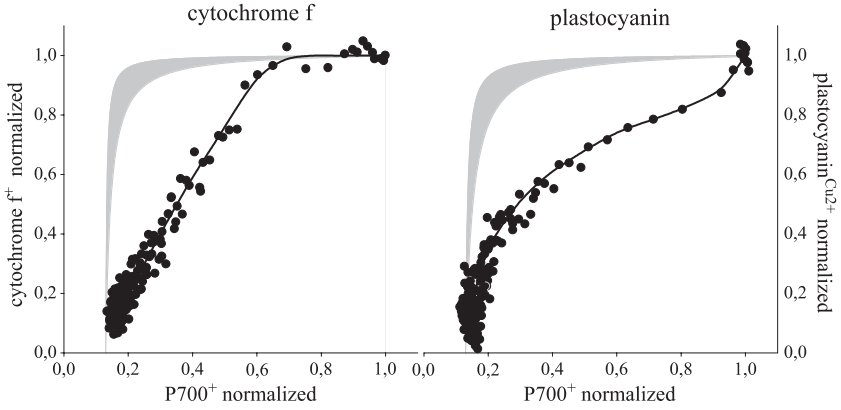

Fig. 2. Equilibrium plots for the components of the 'high potential chain' in stacked thylakoids with maximal electron transport rate. Relaxation signals after the light pulse (see Fig. 1, right) of cytochrome *f*, PC and P_{700} were normalized and plotted against each other. The grey area indicate the expected behaviour calculated from the midpoint potentials given in this figure with:

$$y = \frac{Ka - a - K}{(a-1)K} \frac{(P_{700} - a)K}{1 - (P_{700} - a) + K(P_{700} - a)}$$

y, normalized $PC^{Cu^{2+}}$ or cytochrome f^+; *K*, equilibrium constant, from Table 2 it follows *K* (PC/P_{700})=43–172 and *K* (cyt *f*/P_{700})=64–312; *a*, point of intersection with the abscissa axis. The parameter *a* represents the slow P_{700}^+ relaxation component. For further details see text.

Table 2
Published values for midpoint potentials (E_m) of components of the 'high potential chain' from spinach

Component	Literature	E_m in mV
Cytochrome *f*	[41–43]	+340 to +360
PC	[23,35]	+355 to +370
Bound to PSI	[35]	+421
P_{700}	[23,35]	+465 to +485
With bound PC	[35]	+475

The equilibrium constant, K_{eq}, is calculated according to $K_{eq}=e^{(-n\,F\,E_m)/(R\,T)}$; n, number of electrons transferred (n=1); F, Faraday constant (96,500 C mol^{-1}); R, gas constant (8.314 J mol^{-1} K^{-1}); T, temperature (293 K).

Furthermore, the plots exhibit a complex shape. This indicates that redox equilibration between the components of the 'high potential chain' is not homogenous throughout the membrane.

3.3. Electron transport rate and redox equilibration

In the analysis shown in Fig. 2 the electron transport rate is at its maximum. The overall rate could be obtained from the P_{700}^+ reduction kinetics after the light pulse. The time constant was 8.8±0.3 ms (n=5). To examine the influence of the electron transport rate from PQH_2 to P_{700} on the K_{app}, the equilibration analysis was carried out in the presence of varying concentrations of DNP-INT, a potent inhibitor of the PQH_2 oxidation at the cyt *bf* complex [27,28]. DNP-INT (1 μM) decreases the P_{700}^+ reduction rate to about 20% of its control value. The corresponding equilibration plots are shown in Fig. 3. Compared to those of the non-inhibited thylakoids (solid line, from Fig. 2), the apparent equilibrium constants between PC/P_{700} and cytochrome *f*/P_{700} are now shifted to much higher values and more or less approximate the expected curves derived from the E_m values (grey areas). Furthermore, the curves are less complex and exhibit a nearly hyperbolic shape, similar as theoretically expected.

The data shown in Fig. 3 were fitted to calculated equilibrium curves. From these fittings, we determined K_{app} values for different inhibition levels adjusted by different DNP-INT concentrations. The insets in Fig. 3 show an inverse correlation between the electron transport rate and the K_{app}. For data fitting, it is noteworthy that at low levels of inhibition the equilibration curves deviate from the ideal hyperbolic shape (see Fig. 2). However, in a first approximation, K_{app} as a function of the electron transport rate can be quantified in this way.

3.4. Membrane stacking and redox equilibration

Redox equilibration was further examined after de-stacking of grana membranes (Fig. 4). De-stacking was obtained by incubating thylakoids in a hypotonic medium with low ionic strength. Under this condition, the time constant for P_{700}^+ reduction (8.0±0.1 ms, n=2) was nearly identical to that of stacked membranes (8.1±0.1 ms). However, the redox equilibration plots differed clearly from those obtained for stacked thylakoid membranes (solid lines). The equilibration curve for de-stacked thylakoids was less complex and significantly closer to the theoretically calculated curves. It suggests that during fast electron transport, in de-stacked membranes the 'high potential chain' was much closer to its equilibrium, compared to intact, stacked thylakoids.

3.5. PC/P_{700} redox equilibration in leaves

The inset of Fig. 5 shows P_{700} and PC redox kinetics measured with an infiltrated leaf disc. The FR measuring light efficiently penetrates the leaf tissue, as there are little FR absorbing components. Infiltration minimizes light scattering of the leaf tissue. As mentioned above, we did not see a slow component in the redox kinetics. We

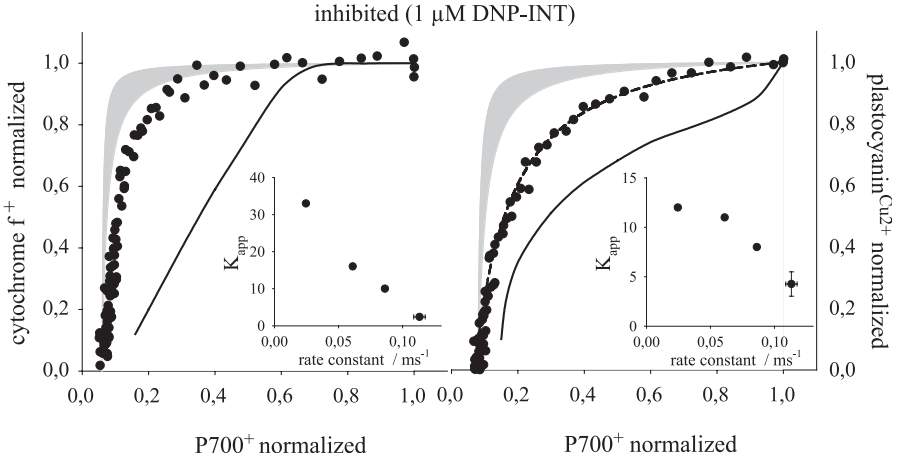

Fig. 3. Equilibrium plots for the components of the 'high potential chain' in stacked thylakoids with slowed down electron transport rate. Thylakoids were incubated in the presence of different concentrations of the cyt *bf* inhibitor DNP-INT (1 μM in this figure). Solid lines are taken from Fig. 2 to clarify the deviations. The dashed line (right) indicates an equilibrium constant of 10 (see Discussion). Insets: the apparent equilibrium constants (K_{app}) were calculated with the equation given in Fig. 2. The actual inhibition was quantified by the P_{700}^+ reduction rate constant and plotted against K_{app}. Note the strong dependence of K_{app} on the rate constant.

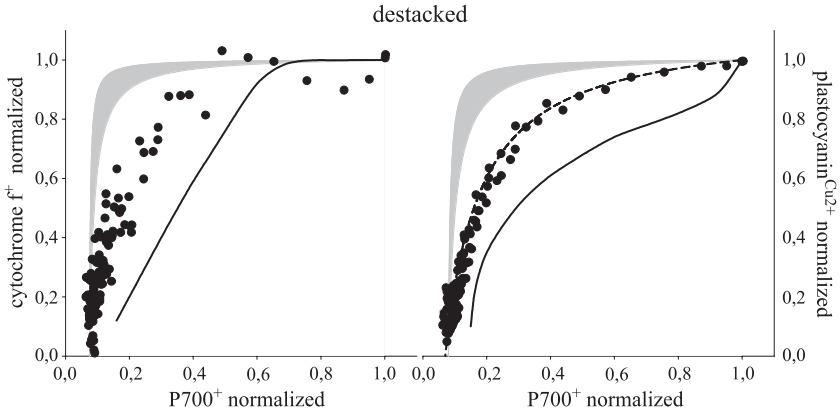

Fig. 4. Equilibrium plots for the components of the 'high potential chain' in de-stacked thylakoids. Thylakoids were incubated for at least 10 min in a de-stacking medium. Solid lines are taken from Fig. 2 to clarify the deviations. For further details see Fig. 3.

determined a PC/P_{700} ratio of 3.64±0.25 (n=10), which was in good agreement to the value determined for isolated thylakoids. Addition of the uncoupler nigericin (10 μM) resulted in a stimulation of the P_{700}^+ reduction time constant from about 26 ms to about 11 ms, which is close to the rate constant found in thylakoids. This can be explained by an acidification of the thylakoid lumen in the light in the absence of the uncoupler leading to a 'photosynthetic control' which slows down the electron flux through the cyt *bf* complex [29,30]. Photosynthetic control is abolished by the uncoupler. One has to take into consideration that the uncoupler could also affect other cellular membranes and stimulate proton leakage from the cell vacuole. However, if this would occur it seems to have only little, if any influence on the electron transport rate. The equilibrium plot PC^+ vs. P_{700}^+ obtained from leaves infiltrated with uncoupler (Fig. 5, closed symbols) are similar to that obtained for intact, non-inhibited thylakoids (compare Fig. 2, right), while the curve from leaves without uncoupler (slow electron flux; Fig. 5, squares) was hyperbolic and similar to that of DNP-INT inhibited (compare Fig. 3, right) or de-stacked (Fig. 4) thylakoids. In thylakoids (Fig. 3, right) as well as in leaf discs (Fig. 5, white squares) K_{app} rises if the electron transport rate decreases and approximates K_{eq}.

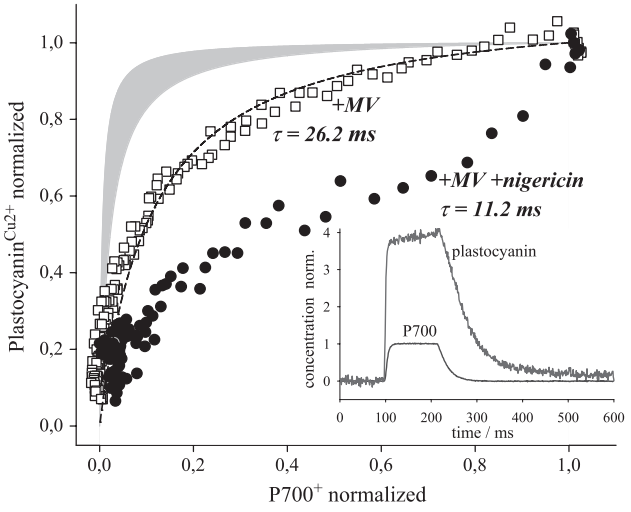

Fig. 5. Equilibrium plots for the redox system PC/P_{700} in infiltrated leaf discs. Leaf discs were infiltrated in the presence of 0.4 mM methylviologen and in the presence (white squares) or absence (black circles) of 10 μM nigericin. The indicated time constants are derived from the P_{700}^+ reduction kinetics. The dashed line indicates an equilibrium constant of 10 (see Discussion). Note the similarities of the equilibrium curves to Fig. 2 right (not inhibited) and Fig. 3 right (inhibited). Inset: deconvoluted P_{700} and PC redox kinetics.

4. Discussion

4.1. A novel method for detecting PC redox kinetics

In the visible spectral region, PC is difficult to measure, due to its broad difference absorption spectrum [23,24] and strong superposition by other redox active chromophores of the photosynthetic electron transport chain [31]. The FR region is favourable because only P_{700}^+, PC^+ and ferredoxin as well as light scattering changes contribute to absorption changes [23]. Measurements around 810 nm were already applied for the registration of the redox status of P_{700} [32–34]. Here, we used a PAM photometer for registration of the difference signal 810–860 nm (mainly P_{700}) and the 810 nm signal (PC and P_{700}). Calibrating the measuring system (Table 1) using PC- and PSI-enriched preparations with well-defined concentrations of chromophores, we deconvolute the FR signals and separate PC and P_{700} signals (Eqs. (1) and (2)). The good agreement between the PC and P_{700} signals obtained from isolated thylakoids and leaf discs suggest that it is a useful spectroscopic approach to investigate PC in leaves.

4.2. PC diffusion limits redox equilibration within the '*high potential chain*'

In a recently published study [35], the ET between isolated PC and PSI (both from spinach) was comprehensively examined. Kinetic data from single-turnover flash experiments were used to develop a model which includes

binding and electron transfer equilibriums. It was an important result of these studies that the electron transfer from PC to P_{700} is optimized by the highly favoured binding of reduced PC to PSI, relative to oxidized PC. At the same time, however, the midpoint redox potential of PC bound to PSI was shifted to a more positive value compared to that of free PC. Thus, the equilibrium constant for the ET chain from PC to the P_{700}^{+} decreases from 85±40 calculated for free PC (Table 2; grey area in Fig. 2, right to Fig. 5, right) to a value of about 10 as determined for the PC–PSI complex [35]. The corresponding equilibration curve calculated for K_{app}=10 is shown as dashed line in Figs. 3–5 (right side). In thylakoids, the situation could be more complex. As PC is in excess (PC/P_{700}=3.60) there may be an equilibration between bound and unbound PC. In that case, the apparent equilibrium constant between P_{700} and PC should be between that expected for the free component and that for the PC–PSI complex and should vary with the oxidation state of the thylakoids (F. Drepper, personal communication). However, in leaf discs and isolated thylakoids under conditions where the ET rate is slowed down by an inhibitor (Figs. 3 and 5), or the electron transport is fast but the grana are de-stacked (Fig. 4), the observed equilibration plots fit closely to the curve calculated for K_{app}=10. It is an indication that under these particular conditions the redox equilibration between PC and P_{700} is mainly determined by the PC–PSI complex, and neither the concentration of free PC^{+} nor the diffusion of PC seem to determine the reaction.

A quite different situation is seen in well stacked thylakoids with fast (non-inhibited) electron transport (Figs. 2 and 5). Here, the equilibration curves are complex and non-hyperbolic and do not fit any of the calculated curves. The curves indicate that K_{app} could have values much smaller than 10, indicating that at least one large fraction of PSI relaxes far from its equilibrium with the high potential chain.

K_{app} values less than 5 were previously observed for the redox equilibrium between cytochrome *f* and P_{700} in light pulse experiments [36,37] and indirectly derived from steady state measurements [38]. Delosme [36] and Joliot and Joliot [37] discussed it in terms of an altered function of the cyt *bf* complex. In this case, however, the redox equilibration between cyt *f* and P_{700} (Fig. 2, left) but not that of PC and P_{700} would be affected. Here, however, we observe a disequilibrium between PC and P_{700} (Fig. 2, right), indicating that the interaction between PC and PSI is disturbed. As the electron transfer within the PC–PSI is fast (10–20 μs, Ref. [3]), diffusion of PC to its docking site could be the factor restricting the equilibration. If the PC diffusion rate is slow compared to other electron transfer rates, cyt f^{+} and PC^{+} would become rapidly reduced while P_{700}^{+} remains oxidized due to restricted PC diffusion, as is seen in Fig. 2. This interpretation of the equilibration curves is supported by the observation that de-stacking brings the PC/P_{700} redox pair closer to its thermodynamic equilibrium (Fig. 4). In de-stacked membranes, the lumen space is widened and potential diffusion barriers could be eliminated. Furthermore, a decrease of the electron flux rate (by DNP-INT or by membrane energization) has a similar effect on the redox equilibration. After inhibition, the electron flux rate could approximate the apparent PC diffusion rate, hence, PC diffusion could no more limit the redox equilibration and K_{app} would approach K_{eq}. It further suggests that the deviation from the thermodynamic equilibrium observed during fast electron transport is caused by a kinetic barrier, most likely PC migration. As the inner width of the thylakoid lumen (approx. 4 nm, [5]) and the size of the PC protein (approx. 4×3×3 nm, [2]) are in the same order, obstructed PC diffusion could be due to non-sufficient width of the diffusion space. Cruz et al. [12] observed that the electron transport is inhibited during osmotic stress (where the lumen width could be further reduced) and explained this observation with a restricted PC mobility in the lumen. A second limiting factor could be protruding proteins, which act as obstacles in the luminal diffusion space [8,11]. In particular, the large water splitting complexes tightly packed in the inner grana membranes could severely restrict the PC lateral mobility in the lumen of grana cores and act as a diffusion barrier between the fraction of cyt *f* located in grana cores and PSI. The two PC docking proteins, cyt *f* and the PsaF subunit could also limit long-distance diffusion.

4.3. Slowly and rapidly equilibrating PC domains

The non-hyperbolic, complex shape of the curves (Fig. 2) suggests that the redox components equilibrate in a non-homogenous way. Part of the cyt *f* versus P_{700} curve in Fig. 2 actually fits well to the theoretical equilibration curve, suggesting that roughly, about 30% of P_{700} equilibrates rapidly with cyt *f*, i.e. PC diffusion should be fast. Only a second, larger fraction relaxes far from the equilibrium. It was assumed [11], that long-range lateral PC diffusion throughout the lumen could be restricted, while short-distance transluminal diffusion between cyt *f* and PsaF located in facing membranes could be fast. Transluminal PC diffusion between cyt *f* and PSI could be of significance in the 'end-lumen' of grana stacks. Here, a stacked membrane packed with PSII and cyt *bf* complexes is located opposite to the non-stacked 'end-membrane' of the granum, which contains a large number of PSI. PC would shuttle the electrons between cyt *f* and PSI over short distances across the lumen, just between facing membranes (see model in Fig. 6). Albertsson [6] presented data demonstrating that about 30% of PSI could be located in end-membranes, but this fraction could be lower in highly stacked grana. To some extent, transluminal PC diffusion could also occur in grana margins. In this sense, the end-lumen and, perhaps, the lumen space in the margins of grana stacks could be regarded as 'rapid PC diffusion domains'. This would agree well with our suggestion that about 30% of PSI equilibrate rapidly with cyt *f* (experiment in Fig. 2A). On the other

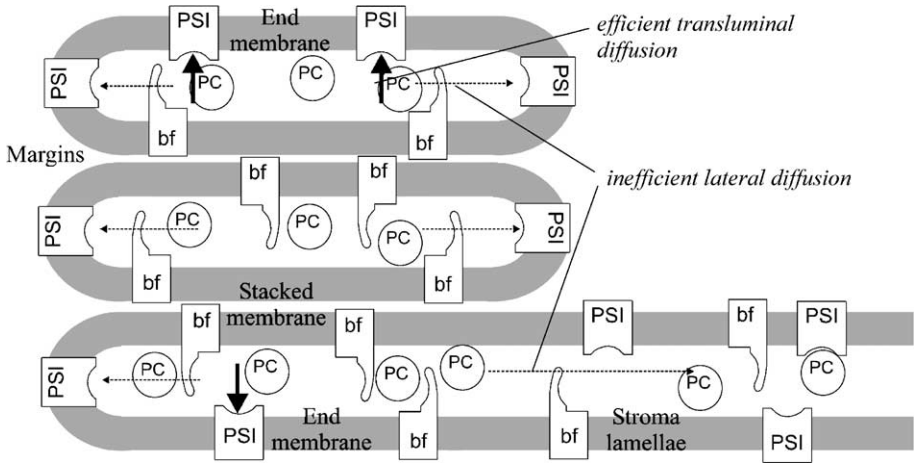

Fig. 6. Model of PC diffusion in the thylakoid membrane. The thylakoid model is based on the model proposed by Albertsson [6]. PSI, Photosystem I; bf, cytochrome *bf* complex; PC, plastocyanin. For clarity, PSII, LHCs and the ATPase are omitted. Light dashed arrows indicate restricted lateral PC diffusion; bold arrows indicate transluminal unrestricted diffusion in the end-membranes of grana thylakoids.

hand, the fraction of cyt *bf* complexes located in these domains (e.g. 15% of total cyt *bf* is located in end-membranes [6]) and, hence, its contribution to the overall electron flux may be rather low. A much larger fraction of cyt *bf* complexes is located in the inner grana membranes, and these complexes could only slowly equilibrate with P_{700}, as they are separated from PSI by long-range lateral PC diffusion pathways (see model in Fig. 6). Assuming random cyt *bf* distribution, 50% of cyf *bf* complexes located in grana stacks may have a mean lateral distance of 60–70 nm to the next PSI in the margins [8]. Lateral 'percolation' of the diffusible PC protein between 'obstacles'—mainly PSII/water splitting complexes—is expected to slow down its diffusion rate with increasing distance. Our experiments suggest that this kind of long-distance PC diffusion controls the redox equilibration rate within the 'high potential chain'.

On the basis of this model (Fig. 6), we explain the kinetics of the dark-relaxation of the 'high potential chain' in the following way: at the end of the light pulse, all components of the 'high potential chain' are oxidized. In a first approximation the subsequent reduction by the plastoquinol pool can be subdivided into two different phases. Phase 1: after the light pulse, one fraction of P_{700}^+ in the end-membranes becomes rapidly reduced (by efficient transluminal PC diffusion; Fig. 6 upper part), while a larger fraction of P_{700}^+ remains oxidized, because of slow lateral PC diffusion from the grana cores. Due to the restricted PC diffusion, a large fraction of PC^+ in the grana core becomes more rapidly reduced than P_{700}^+. The first phase is completed approx. 10 ms after the light pulse (estimated from comparing the equilibration curves in Fig. 2 with the relaxation kinetics). Phase 2: P_{700}^+ in the end-membrane (about 30%) is already reduced. P_{700}^+ in the margins and stroma lamellae (about 70%) becomes more slowly reduced via lateral PC diffusion from the grana core. Concomitantly, PC^+ in the grana will be further reduced. After substantial reduction of the PC pool (about 3–4 PC per PSI, 8–10 per cyt *f*) reduction of cyt f^+ starts (Fig. 2, left, middle and lower left part of the curve). Similarly, the slow phase in the PC photooxidation kinetics (Fig. 1) could represent a slowly diffusing PC fraction migrating from the inner core of the grana to the PSI containing margins.

4.4. Physiological implications

The most significant consequence of restricted long range PC diffusion is a slow redox equilibration between grana and stroma lamellae: electrons extracted from water at PSII are kept in the grana. There is good evidence that the second diffusible carrier, PQ also does not rapidly equilibrate throughout the membrane [19,39]. Obviously, rapid PQ equilibration is restricted to small 'diffusion domains' within the grana, while its long-range diffusion is slow. Consequently, in high light the PQ pool in the grana core remains reduced, while that of the distant stroma lamellae remains oxidized. Taking these observations together, it seems clear that electron shuttling from grana to stroma lamellae is restricted. It has been discussed that cyclic electron transport is located in the stroma lamellae [6,40]. Protection of stroma lamellae against 'overreduction' by electron flow from the (PSII-containing) grana core is an important requirement to keep appropriate redox poise for a proton pumping cyclic electron transport [6,15,40].

However, restricted PC migration may also be of significance for the flux control of the linear electron transport. If lateral PC diffusion from grana to PSI in the margins and stroma lamellae is restricted, the number of PC could be an important factor controlling the linear electron flux. Under metabolic conditions, where photosynthesis is controlled by the electron-consuming carbon reactions, restriction of electron flux through the high potential chain could prevent 'overreduction' of PSI and related production of reactive oxygen species. In fact, the *petE* (PC) gene expression is under metabolic control [16,17]. In a

subsequent paper, we will demonstrate a significant contribution of PC to the flux control on the photosynthesis in leaves.

Acknowledgment

H.K is supported by the Deutsche Forschungsgemeinschaft. M.A.S. is supported by the "Studienstiftung des Deutschen Volkes". The authors thank Dr. Friedel Drepper for helpful discussion.

References

[1] S. Katoh, Early research on the role of plastocyanin in photosynthesis, Photosynth. Res. 76 (2003) 255–261.
[2] J.M. Guss, P.R. Harrowell, M. Murata, V.A. Norris, H.C. Freeman, Crystal structure analysis of reduced (Cu^{I}) poplar plastocyanin at six pH values, J. Mol. Biol. 192 (1986) 361–387.
[3] A.B. Hope, Electron transfers amongst cytochrome *f*, plastocyanin and photosystem I: kinetics and mechanisms, Biochim. Biophys. Acta 1456 (2000) 5–26.
[4] K. Sigfridsson, Plastocyanin, an electron-transfer protein, Photosynth. Res. 57 (1998) 1–28.
[5] P.-O. Arvidsson, C. Sundby, A model for the topology of the chloroplast thylakoid membrane, Aust. J. Plant Physiol. 26 (1999) 687–694.
[6] P.-A. Albertsson, A quantitative model of the domain structure of the photosynthetic membrane, Trends Plant Sci. 6 (2001) 349–354.
[7] L.A. Staehelin, G.W.M. van der Staay, Structure, composition, functional organization and dynamic properties of thylakoid membranes, in: D.A. Ort, C.F. Yocum (Eds.), Oxygenic Photosynthesis: The Light Reactions, Kluwer Academic Publishers, Netherlands, 1996, pp. 11–30.
[8] J. Whitmarsh, Mobile electron carriers in thylakoids, in: A. Pirson, M.H. Zimmermann (Eds.), Encyclopedia of Plant Physiology, vol. 19, Springer Verlag, Berlin, 1986, pp. 508–525.
[9] S. Murakami, S. Packer, Protonation and chloroplast membrane structure, J. Cell Biol. 47 (1970) 332–351.
[10] W. Haehnel, R. Ratajczak, H. Robenek, Lateral distribution and diffusion of plastocyanin in chloroplast thylakoids, J. Cell Biol. 108 (1989) 1397–1405.
[11] W. Haehnel, Photosynthetic electron transport in higher plants, Annu. Rev. Plant Physiol. 35 (1984) 659–693.
[12] J.A. Cruz, B.A. Salbilla, A. Kanazawa, D.A. Kramer, Inhibition of plastocyanin to $P700^{+}$ electron transfer in *Chlamydomonas reinhardtii* by hyperosmotic stress, Plant Physiol. 127 (2001) 1167–1179.
[13] J. Nield, M. Balsera, J.D.L. Rivas, J. Barber, Three-dimensional electron cryo-microscopy study of the extrinsic domains of the oxygen-evolving complex of spinach, J. Biol. Chem. 277 (2002) 15006–15012.
[14] D. Stoebel, Y. Choquet, J.-L. Popot, D. Picot, An atypical haem in the cytochrome b_6f complex, Nature 426 (2003) 413–418.
[15] J.F. Allen, Cyclic, pseudocyclic and noncyclic photophosphorylation: new links in the chain, Trends Plant Sci. 8 (2003) 15–19.
[16] J.C. Gray, J.A. Sullivan, J.-H. Wang, C.A. Jerome, D. McLean, Coordination of plastid and nuclear gene expression, Philos. Trans. R. Soc. Lond., B 358 (2002) 135–145.
[17] T. Pfannschmidt, Chloroplast redox signals: how photosynthesis controls its own genes, Trends Plant Sci. 8 (2003) 33–41.
[18] P.J. Randall, D. Bouma, Zinc deficiency, carbonic anhydrase, and photosynthesis in leaves of spinach, Plant Physiol. 52 (1973) 229–232.
[19] H. Kirchhoff, S. Horstmann, E. Weis, Control of the photosynthetic electron transport by PQ diffusion microdomains in thylakoids of higher plants, Biochim. Biophys. Acta 1459 (2000) 148–168.
[20] R.J. Porra, W.A. Thompson, P.E. Kriedermann, Determination of accurate absorption coefficient and simultaneous equations for essaying chlorophylls *a* and *b* extracted with four different solvents: verification of the concentration of chlorophyll standards by atomic absorption spectroscopy, Biochim. Biophys. Acta 975 (1989) 384–394.
[21] J.E. Mullet, J.J. Burke, C.J. Arntzen, Chlorophyll proteins of photosystem I, Plant Physiol. 65 (1980) 814–822.
[22] P.V. Sane, G.A. Hauska, The distribution of photosynthetic reactions in the chloroplast lamellar system: I. Plastocyanin content and reactivity, Z. Naturforsch. 27b (1972) 932–938.
[23] C. Klughammer, U. Schreiber, Analysis of light-induced absorbance changes in the near-infrared spectral region, Z. Naturforsch. 46C (1991) 233–244.
[24] S. Katoh, Plastocyanin, in: A. Trebst, M. Avron (Eds.), Encyclop. Plant Physiol., Photosynthesis I, vol. 5, Springer Verlag, Berlin, 1977, pp. 247–252.
[25] C. Klughammer, U. Schreiber, Measuring P700 absorbance changes in the near infrared spectral region with a dual wavelength pulse modulation system, in: G. Garab (Ed.), Photosynthesis: Mechanism and Effects, vol. 5, Kluwer Academic Publi, Netherlands, 1998, pp. 4357–4360.
[26] T. Fujii, E. Yokoyama, K. Inoue, H. Sakurai, The sites of electron donation of photosystem I to methyl viologen, Biochim. Biophys. Acta 1015 (1990) 41–48.
[27] A. Trebst, H. Wietoska, W. Draber, H.J. Knops, The inhibition of photosynthetic electron flow in chloroplasts by the dinitrophenylether of bromo- or jodo-nitrothymol, Z. Naturforsch. 33c (1978) 919–927.
[28] E. Lam, The effects of quinone analogues on cytochrome b_6 reduction and oxidation in a reconstituted system, Fed. Eur. Biochem. Soc. 172 (1984) 255–260.
[29] B. Rumberg, U. Siggel, pH changes in the inner phase of the thylakoids during photosynthesis, Naturwissenschaften 56 (1969) 130–132 (Heft 3).
[30] Y. Kobayashi, Y. Inoue, K. Shibata, U. Heber, Control of electron flow in intact chloroplasts by the intrathylakoid pH, not by the phosphorylation potential, Planta 146 (1979) 481–486.
[31] H.T. Witt, Charge separation in photosynthesis, in: H. Gerischer, J.J. Katz (Eds.), Light-Induced Charge Separation in Biology and Chemistry, Verlag Chemie, 1979, pp. 303–330.
[32] E. Weis, J.T. Ball, J. Berry, Photosynthetic control of electron transport in leaves of *Phaseolus vulgaris*: evidence for regulation of photosystem 2 by the proton gradient, in: J. Biggens (Ed.), Prog. Photosynth. Res., vol. II, Martinus Nijhoff Publishers, Dordrecht, 1987, pp. 11.553–11.556.
[33] J. Harbinson, F.I. Woodward, The use of light-induced absorbance changes around 820 nm to monitor the oxidation state of P-700 in leaves, Plant Cell Environ. 10 (1987) 131–140.
[34] U. Schreiber, C. Neubauer, C. Klughammer, Devices and methods for room-temperature fluorescence analysis, Philos. Trans. R. Soc. Lond., B 323 (1989) 241–251.
[35] F. Drepper, M. Hippler, W. Nitschke, W. Haehnel, Binding dynamics and electron transfer between plastocyanin and photosystem I, Biochemistry 35 (1996) 1282–1295.
[36] R. Delosme, Electron transfer from cytochrome f to photosystem I in green algae, Photosynth. Res. 29 (1991) 45–54.
[37] P. Joliot, A. Joliot, Electron transfer between the two photosystems: II. Equilibrium constants, Biochim. Biophys. Acta 765 (1984) 219–226.
[38] P.H. van Vliet, J. Harbinson, Modelling stead state P700 photooxidation in leaves: the role of plastocyanin, in: N. Murata (Ed.), Research in Photosynthesis, vol. II, Kluwer Academic Publishers, Netherlands, 1992, pp. 527–530.

[39] J. Lavergne, J.-P. Bouchaud, P. Joliot, Plastochinone compartimentation in chloroplasts: II. Theoretical aspects, Biochim. Biophys. Acta 1101 (1992) 13–22.
[40] P. Joliot, D. Béal, A. Joliot, Cyclic electron flow under saturating excitation of dark-adapted *Arabidopsis* leaves, Biochim. Biophys. Acta 1656 (2004) 166–176.
[41] E. Hurt, G. Hauska, Identification of polypeptides in the cytochrome b_6f complex from spinach chloroplasts with redox-center-carrying subunits, J. Bioenerg. Biomembranes 14 (1982) 405–424.
[42] A.B. Hope, The chloroplast cytochrome *bf* complex: a critical focus on function, Biochim. Biophys. Acta 1143 (1993) 1–22.
[43] S.U. Metzger, W.A. Cramer, J. Whitmarsh, Critical analysis of the absorption coefficient of chloroplast cytochrome *f*, Biochim. Biophys. Acta 1319 (1997) 233–241.